

Strain Patterns and Strain Accumulation Along Plate Margins

J. C. Savage
U.S. Geological Survey, 345 Middlefield Road
Menlo Park, California 94025

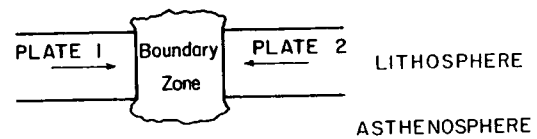
Abstract. Observations of strain accumulation along plate margins in Japan, New Zealand, and the United States indicate that: 1) a typical maximum rate of secular strain accumulation is on the order of 0.3 ppm/a, 2) a substantial part of the strain accumulation process can be attributed to slip at depth on the major plate boundary faults, and 3) some plastic deformation in a zone 100 km or more in width is apparently involved in the strain accumulation process.

Introduction

Repeated geodetic surveys along plate margins show gradual changes imposed by the motion of plates as well as abrupt changes occurring at the time of great earthquakes. Secular changes in angles within a triangulation network may amount to 6 arcseconds/century or more, and 10-km lines in a trilateration network may change length at a rate of 0.3 m/century or more. Probably the best way to display the changes observed in geodetic networks is by means of the inferred strain field. The strain field is preferred to the displacement field for two reasons: 1) Strain is calculated from the local changes and does not involve accumulation and propagation of errors across the network. 2) The displacement field is generally ambiguous to the extent that the relative translation and rotation of the two surveys is uncertain. The general procedure for calculating strain is to treat a network as a whole or some subsection of it as subject to uniform strain, and then to find the uniform strain field that best accounts for the observed changes in angles (triangulation) or length (trilateration). Because scale in triangulation is somewhat less certain than angles, it is probably best to calculate only the shear components $\gamma_1 = e_{xx} - e_{yy}$ and $\gamma_2 = 2e_{xy}$ directly from the angle changes rather than attempt to calculate the complete surface strain field. (Notice that the shear components are given in engineering shear, twice the tensor shear.) Schemes for calculating strain from triangulation data have been described by Frank (1966) and Prescott (1976). For trilateration data a scheme similar to that used by Scholz and Fitch (1969) is recommended. The data should be sufficiently redundant such that not only can the strain components be determined but also reasonable estimates of the standard errors in those components.

The mode of strain accumulation along a plate boundary depends to a large extent upon the nature of the plate boundary. In the simplest model the plate boundary is thought of as a zone several hundred kilometers wide that accommodates relative plate motion by continuously distributed deformation (Figure 1). At a convergent boundary

CONVERGENT PLATE BOUNDARY



TRANSCURRENT PLATE BOUNDARY

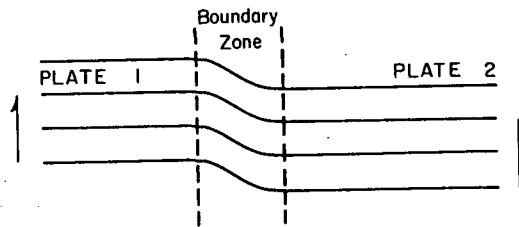


Fig. 1. Plastic boundary zone at the plate margin. The upper figure shows a vertical section across a convergent boundary, and the lower figure shows a plan view of a transcurrent boundary.

this zone would be squeezed horizontally and perhaps thickened vertically, whereas at a transcurrent boundary the zone would undergo distributed shear parallel to the boundary. More elaborate representations of plate-boundary accommodation generally involve gradual slip at depth on great plate-boundary faults with occasional abrupt seismic slip on the upper reaches of the fault. Such representations are based upon dislocation models of faulting (Chinnery, 1961; Freund and Barnett, 1976). A dislocation model for a convergent plate boundary is shown in Figure 2 where the strain released by a major thrust earthquake at a plate boundary is shown. The strain release in that figure is calculated for a constant reverse slip of 1 m over the entire width W of a two-dimensional fault (infinite length perpendicular to the plane of the paper in Figure 2). Because the actual slip on a fault is not constant but presumably varies smoothly, the actual strain profile would be a somewhat smoothed version of the profile in Figure 2. For this reason the short interval of contraction (negative strain) in Figure 2 probably would not be observed. Because W is typically 100 km or so and the slip in a major earthquake perhaps 5 m, the strain release may exceed 20 μ strain over distances of several hundred kilometers. In the period between great earthquakes, an amount of strain equal to that released coseismically must accumulate. Thus, the strain accumulation rate should on the

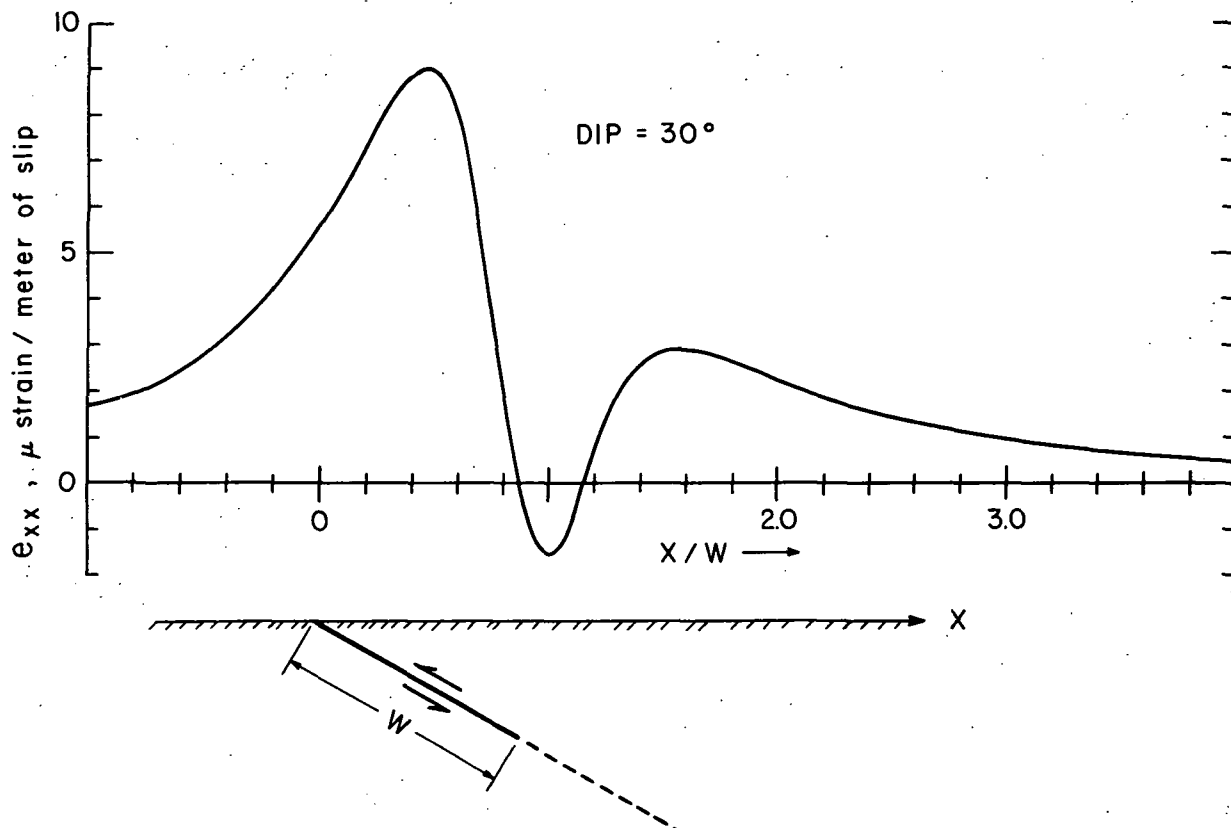


Fig. 2. Dislocation model of a convergent plate margin. The upper sketch shows the strain release by slip on the thrust fault shown in the lower sketch.

average be equal to (but opposite in sign from) the quotient strain release divided by time between earthquakes. This accumulation is presumably due to slip on the deeper sections of the fault that did not slip at the time of the earthquake. Figure 3 shows the equivalent model for strain accumulation at a transcurrent plate boundary. In this figure the strain accumulation (top center) has been calculated for slip at depth on the fault (top left). The earthquake is represented by the abrupt transformation from the configuration shown at the top of the figure to that at the bottom. A striking difference between the two models (Figures 2 and 3) is that strain accumulation is concentrated very close to the plate boundary in the transcurrent model whereas it is broadly distributed at the convergent boundary.

Japan

Figure 4 shows the total shear component $\gamma = (\gamma_1^2 + \gamma_2^2)^{1/2}$ accumulated in Japan during the interval 1900-60. In that figure the magnitude of the total shear component is represented by the length of the bar symbol and the direction of the bar indicates the strike of the plane of maximum shear. (If the plane of maximum left-lateral shear is shown, a solid bar is used;

if the plane of maximum right-lateral shear is shown, a dashed bar is used. In either case one symbol may be replaced by the other symbol drawn perpendicular to the first.) The direction of the axis of maximum contraction is 45° counter-clockwise from the solid bars and 45° clockwise from the dashed bars. Recall that Figure 4 shows the net strain accumulation during the 1900-60.

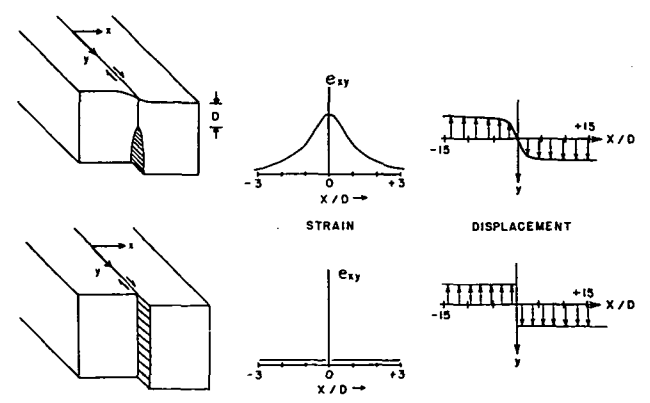


Fig. 3. Dislocation model of a transcurrent plate margin. Strain (top center) accumulates in response to slip at depth on the fault (top left). An earthquake releases the strain (lower sketches).

Several major earthquakes occurred in Japan during that period, and the strain released in those seismic events locally dominates the total accumulation of strain. This circumstance has introduced some complexity into the patterns shown in Figure 4.

We will discuss here only the south coast of Japan between longitudes 133°E and 140°E, the region of interaction with the Philippine Sea plate. That plate underthrusts Japan in a generally northwest direction resulting in a uniaxial northwest-southeast compression (solid bars north-south or dashed bars east-west). Stress release by a major earthquake results in a local uniaxial northwest-southeast extension (solid bars east-west and dashed bars north-south). With this background, it is easy to interpret the strain accumulation along the south coast of Japan in Figure 4. Only in the Tokai district (longitude 138°E) and perhaps extreme western Shikoku (longitude 133°E) is the expected northwest-southeast compression apparent. Elsewhere along the south coast there is a northwest-southeast extension corresponding to strain relief by the great 1946 Nankaido (longitude 134°E), 1944 Tonankai (longitude 136°E), and 1923 Kanto (longitude 140°E) earthquakes. It is not hard to see why the Japanese are presently concerned about an earthquake hazard in the Tokai district. Although the strain measurements are quite consistent with the dislocation model of Figure 2, the possibility that some of the accommodation occurs by anelastic deformation distributed over a broad boundary zone (Figure 1) is not excluded. Measurements of strain accumulation and release over several earthquake cycles could identify the relative contribution of continuous anelastic deformation and discrete dislocation motion.

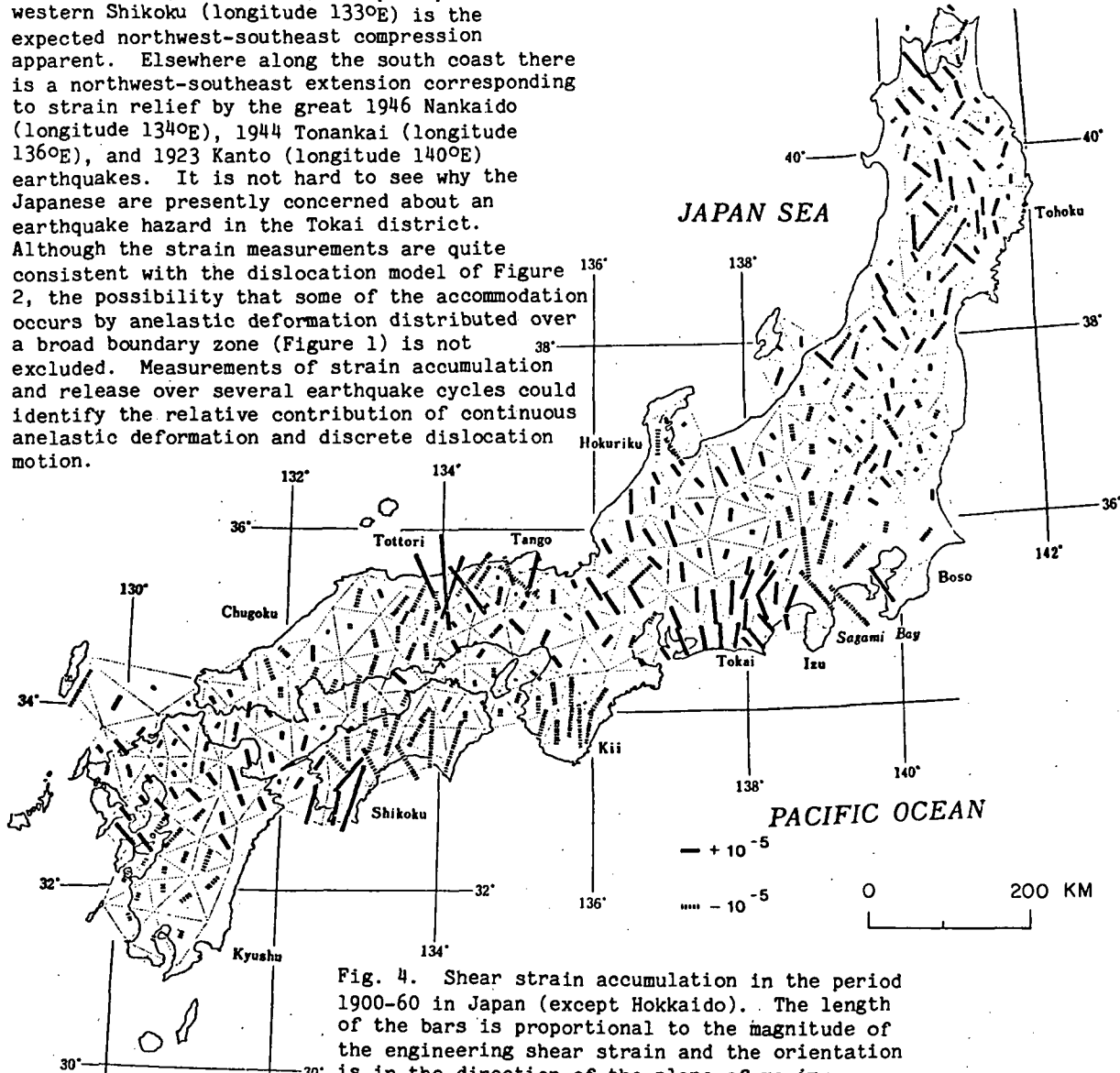


Fig. 4. Shear strain accumulation in the period 1900-60 in Japan (except Hokkaido). The length of the bars is proportional to the magnitude of the engineering shear strain and the orientation is in the direction of the plane of maximum left-lateral shear for the solid bars and right-lateral shear for the dashed bars. (From Harada and Kassai, 1971).

New Zealand

As a second example we consider the deformation in New Zealand as described by Walcott (1978a). New Zealand lies along the Pacific-Indian plate boundary about 1500 km north of the present pole of relative plate rotation. Because of the proximity of the pole of rotation, the relative motion of the Pacific and Indian plates changes from approximately normal convergence at the rate of 50 mm/a (Pacific plate being underthrust) on North Island to highly oblique convergence at the rate of 40 mm/a (Indian plate being underthrust) on South Island.

The rate of strain accumulation in New Zealand as determined from triangulation data by Walcott (1978a) is shown in Figure 5. (Notice that in Figure 5 the bar indicates the direction of the axis of greatest contraction rather than the

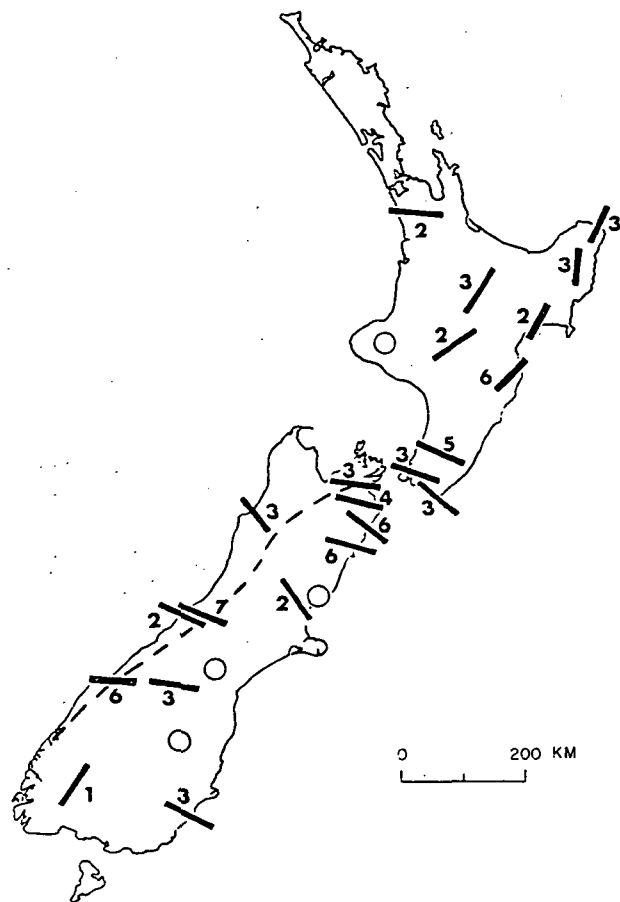


Fig. 5. Rate of shear strain accumulation in New Zealand as given by Walcott (1978a). The bars are in the direction of maximum compression, and the magnitude of the engineering shear strain in units of $10^{-7}/a$ is given by the number beside the bar. Open circles indicate regions where no significant strain rate was observed. The dashed line running the length of the South Island shows the position of the Alpine fault.

strike of the plane of maximum shear as in Figure 4). These strain rates represent the average rate of accumulation over periods generally in excess of 60 years and in some cases may include strain release associated with major earthquakes, as in northeastern New Zealand, site of the 1931 Hawke's Bay earthquake (Walcott, 1978b). There the shear strain (Figure 5) shows a northwest-southeast extension typical of strain release rather than compression expected for a convergent boundary. In central New Zealand the compression axis is approximately normal to the plate boundary as expected for convergence of the Pacific and Indian plates. In the southern part of New Zealand the compression axis has rotated counterclockwise so that the relative plate motion is oblique to the plate boundary along the Alpine fault. The strain accumulation rates are also quite consistent with the plate tectonics model. As shown in Figure 5 the strain accumulation appears to average about 0.3

$\mu\text{strain}/a$ across a zone perhaps 200-km wide, implying relative motion of about 60 mm/a. Such continuously distributed deformation is, of course, implied by the models in Figure 1. The observations on North Island where plate convergence is dominant could also be explained by the model of Figure 2 which provides for a broad distribution of strain. Superficially at least, the observations of a broad distribution of strain on South Island would appear to exclude the transcurrent boundary model of Figure 3. However, there is some evidence that the strain in South Island is appreciably concentrated along the Alpine fault. For example, the two adjacent strain determinations of 0.2 and 0.7 $\mu\text{strain}/a$ (2 and 7 in units of the figure) on the central west coast of South Island in Figure 5 represent measurements solely on the western fault block (0.2 $\mu\text{strain}/a$) and spanning the Alpine fault (0.7 $\mu\text{strain}/a$), respectively. The appreciably higher strain rate in the latter case indicates that a major part of the plate motion is accommodated by slip on the Alpine fault in that area.

United States

The San Andreas fault in California is presumed to define the transcurrent boundary between the Pacific and North American plates. Measurements of strain accumulation in central California, where the San Andreas fault is reasonably straight and closely parallel to the direction of relative plate motion, are shown in Figure 6. Because the measurements shown in that figure are based upon trilateration surveys, the complete strain tensor including dilatation may be calculated. On the average the strain is a shear parallel to the fault and of magnitude about 0.3 $\mu\text{strain}/a$ engineering shear. (The tensor shear is half as large.) The breadth of the shear zone is somewhat greater than might be expected from the model of Figure 3, perhaps partly because accommodation of plate movement is distributed over several subparallel faults. However, even the sum of the motion on the faults seems to be perhaps 30 percent less than the anticipated plate motion; whether the missing 30 percent of the motion is accommodated on offshore faults or distributed over a broad anelastic zone is not known.

Along a 100-km-long straight section of the San Andreas fault south of the Gavilan net (Figure 6), the plate motion is particularly simple. No appreciable strain accumulation is measured on either side of the San Andreas fault, and the entire relative motion appears to be accommodated by steady slip on the fault as shown in the lower diagrams of Figure 3. The relative plate movement measured directly over a zone a few kilometers in width is about 32 mm/a (Savage and Burford, 1973), a value substantially below the 55 mm/a estimated for relative plate motion averaged over the last 4 Ma. The discrepancy may indicate that another fault system, perhaps offshore, accounts for part of the relative plate motion or alternatively that a very broad plastic zone (Figure 1, lower) may be involved.

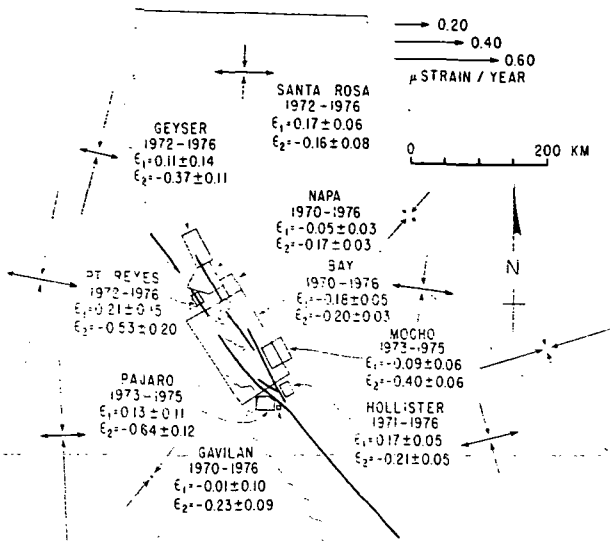


Fig 6. Average principal tensor strain accumulation rates along the San Andreas fault system (heavy lines) in central California for the period 1970-76. The strain rates shown are averages over the areas shown in the associated polygon. The units are strain/a; e_1 denotes the most tensile strain rate, and e_2 the most compressive strain rate. (From Prescott *et al.*, 1978).

The plate boundary is somewhat more complicated in southern California. There the San Andreas fault exhibits a major bend so that an element of plate convergence is introduced. In spite of the bend in the plate boundary, the strain accumulation pattern is remarkably

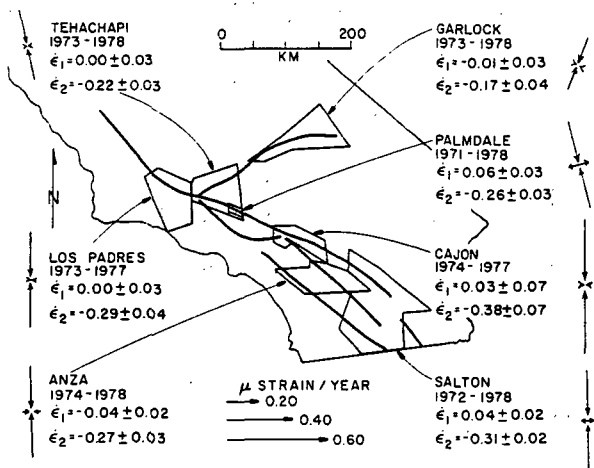


Fig. 7. Average principal tensor strain accumulation rates along the San Andreas fault system (heavy lines) in southern California for the period 1971-78. The strain rates shown are averages over the area shown in the associated polygon. The units are strain/a; e_1 denotes the most tensile strain rate, and e_2 the most compressive strain rate (From Savage *et al.*, 1978).

simple: essentially a uniaxial north-south contraction over a broad region as shown in Figure 7. The origin of this strain field is as yet unexplained. It may be a short-term aberration in the secular strain accumulation as the period of measurement spans only five years.

References

- Chinnery, M. A., The deformation of the ground around surface faults, *Bull. Seismol. Soc. Am.*, **51**, 355-372, 1961.
- Frank, F. C., Deduction of earth strain from survey data, *Bull. Seismol. Soc. Am.*, **56**, 35-42, 1966.
- Freund, L. B., and D. M. Barnett, A two dimensional analysis of surface deformation due to dip slip faulting, *Bull. Seismol. Soc. Am.*, **66**, 667-675, 1976.
- Harada, T., and A. Kassai, Horizontal strain of the crust in Japan for the last 60 years (in Japanese), *J. Geodetic Soc. Japan*, **17**, 4-7, 1971.
- Prescott, W. H., An extension of Frank's method for obtaining crustal shear strains from survey data, *Bull. Seismol. Soc. Am.*, **66**, 1847-1853, 1976.
- Prescott, W. H., J. C. Savage, and W. T. Kinoshita, Strain accumulation rates in the western United States between 1970 and 1978, *J. Geophys. Res.*, (in press), 1978.
- Savage, J. C., and R. O. Burford, Geodetic determination of relative plate motion in central California, *J. Geophys. Res.*, **78**, 832-845, 1973.
- Savage, J. C., W. H. Prescott, M. Lisowski, and N. King, Strain in southern California: measured uniaxial north-south regional contraction, *Science*, (in press), 1978.
- Scholz, C. H., and T. J. Fitch, Strain accumulation along the San Andreas fault, *J. Geophys. Res.*, **74**, 6649-6666, 1969.
- Walcott, R. I., Present tectonics and late Cenozoic evolution of New Zealand, *Geophys. J. Roy. Astr. Soc.*, **52**, 137-164, 1978a.
- Walcott, R. I., Geodetic strains and large earthquakes in the axial tectonic belt of North Island, New Zealand, *J. Geophys. Res.*, **83**, 4419-4429, 1978b.